ARCHIVES OF ELECTRICAL ENGINEERING VOL. 61(1), pp. 33-46 (2012)

DOI 10.2478/v10171-012-0003-5

Iron loss and eddy-current loss analysis in a low-power BLDC motor with magnet segmentation*

ADRIAN MŁOT[1], MARIUSZ KORKOSZ[2], MARIAN ŁUKANISZYN[1]

[1]*Faculty of Electrical Engineering, Automatic Control and Informatics*
Opole University of Technology
Luboszycka 7, 45-036 Opole, Poland

[2]*Rzeszow University of Technology*
W. Pola 2, 35-959 Rzeszów, Poland

e-mail: m.lukaniszyn@po.opole.pl

(Received: 29.08.2011, revised: 09.01.2012)

Abstract: This paper considers a Brushless Direct Current (BLDC) machine prototype with six poles and 36 stator slots including a three phase double-layered distributed winding. Presented modifications of rotor construction are identified in order to achieve the best possible compromise of eddy-current losses and cogging torque characteristics. The permanent magnet (PM) eddy-current loss is relatively low compared with the iron loss; it may cause significant heating of the PMs due to the relatively poor heat dissipation from the rotor and it results in partial irreversible demagnetization. A reduction in both losses is achieved by magnet segmentation mounted on the rotor. Various numbers of magnet segmentation is analysed. The presented work concerns the computation of the no-load iron loss in the stator, rotor yoke and eddy-current loss in the magnets. It is shown that the construction of the rotor with segmented magnets can significantly reduce the PM loss (eddy-current loss). The eddy-current loss in PMs is caused by several machine features; the winding structure and large stator slot openings cause flux density variations that induce eddy-currents in the PMs. The effect of these changes on the BLDC motor design is examined in order to improve the machine performance. 3-D finite-element analysis (FEA) is used to investigate the electromagnetic behaviour of the BLDC motor.

Key words: BLDC motor, iron loss, eddy current losses, permanent magnet segmentation, cogging torque reduction, magnet layers

1. Introduction

Certain industrial applications require BLDC machines. When cost constraints are imperative, designers are forced to use the standard laminations, available on the market. Dif-

* This is extended version of a paper which was presented at the 47th International Symposium on Electrical Machines SME 2011, Szczecin, Poland.

ferent magnetic materials cause different amounts of loss. Knowledge of this loss is important in the analysis of PM machines, due to their complicated structure and the rotational behaviour of their magnetic fields [1-3]. When designing a motor an appropriate combination of the stator teeth per pole and per phase should be used. A bad choice can be a reason of significant iron loss even in the rotor.

The BLDC motor losses are mainly the winding copper loss and iron loss. The winding loss due to eddy-currents is difficult to analyse owning to the complex distribution of 3-phase windings. Hence, winding loss is not considered in this paper. Furthermore, the stator teeth and back iron can also have significant loss due to flux reversals. Knowledge of the iron flux density and its harmonic spectrum allows the loss of the stator core to be estimated.

The permanent magnets and rotor back iron are exposed to low variations in flux and therefore do not generate a significant loss compared with the loss generated by the stator core. Nevertheless, this paper presents 3-D computations of the no-load magnet loss and the iron loss of a prototype BLDC machine. Modifications are based on dividing the PM-poles into multiple magnet segments. This construction of the rotor reduces the eddy-current loss in the PMs and changes slightly the quantities such as electromagnetic torque and ripple torque compared with a conventional rotor with no magnets' segmentation. The cogging torque of PM motor arises from the interaction between rotor magnet and its slotted stator. It has detrimental effects on the motor operation performances, creating speed perturbation, positioning error, vibration, and finally noise. The cogging torque is the main component of the parasitic torque in the BLDC motor considered. This cogging effect is high and can be reduced using the skewed multi-layer PM segments method [4-6].

2. Prototype of BLDC motor

A 6-pole BLDC motor with a modified rotor is considered. The motor has a low mechanical power, 0.55 kW at the rated speed of 1000 rpm. The rated nominal current and voltage is 10 A and 45 V, respectively. Figure 1 shows the test bench including a prototype with the non-segmented magnets.

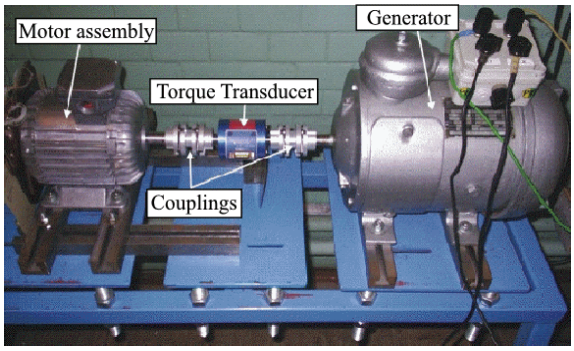

Fig. 1. Test bench of 6-pole 36-slot BLDC motor; the BLDC 0.55 kW machine is coupled to a generator to simulate a loaded operation

The structure of this prototype with calculation and measurements of the no-load torque, cogging torque and EMF were presented in [4, 7]. The stator of the prototype was made of

laminated iron (sheet type EP 600-50A). The rotor is made of solid iron (ST-3 B-H characteristic) with surface mounted PMs which have the shape of cylindrical sections and are magnetized radially.

A finite element model which considers several modifications to the prototype is presented in the next sections. The stator sheet material was changed for 0.5 mm M470-50A steel lamination that is typically used in induction motors (Fig. 2). The next modification is to use different numbers of rotor magnet segments.

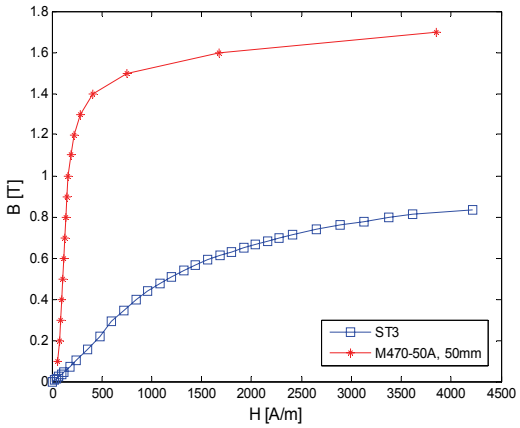

Fig. 2. B-H curve of stator core (M470-50A) and rotor core (ST3) materials

The winding used in the BLDC motor is fed with a rectangular current waveform in the 120 deg. conduction mode, thus only two phases can be supplied simultaneously. Figure 3 shows the distributed integral three-phase double-layer winding used in the motor.

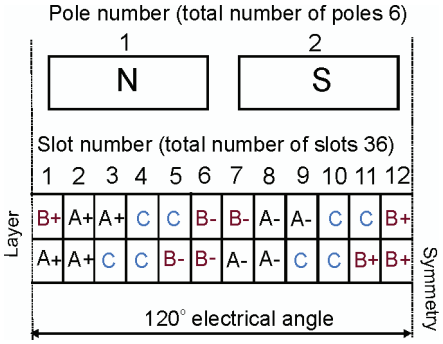

Fig. 3. Diagram of the three phase double-layer distributed winding

The number of slots per pole and phase is integral and equal to 2. In Table 1 common parameters of BLDC PM motor prototype is shown.

The presented prototype (Fig. 1) is constructed for low-speed operation with a low number of turns per phase ($N_t = 5$). Additionally, the stator has small slot openings. The structure of the BLDC motor produces low eddy-current loss in the magnets and in the rotor of up to several percent relative to mechanical power.

Table 1. Selected performance specifications of BLDC PM motor prototype

Description	Value
Air-gap length	1.5 mm
PM material	Sintered NdFeB
PM radial thickness	3 mm
Stator outer diameter	60 mm
Stator and rotor stack length	59 mm
Stator phase resistance	0.34 Ω
Arc width of PM pole	47°
Residual flux density	1.21 T
Coercive magnetizing intensity	829 kA/m^3
Rated nominal current	10 A
Rated power	0.55 kW

3. Losses determination

3.1. Iron losses

Iron loss determination requires knowledge of the magnetic material characteristics for all of the different magnetic motor components. Iron losses comprise three components: eddy-current loss, hysteresis loss and excess loss [2, 3, 8]. Hysteresis loss is an effect that occurs within the ferromagnetic materials. Hence, material selection is minimising the core loss.

Various methods have been proposed in the literature to calculate iron loss [2, 3, 8-11]. One of these methods is the modified Steinmetz equation presented in [9, 10], that predicts losses when waveforms are non-sinusoidal. In the case of sinusoidal excitation (which is typical for form-factor-controlled Epstein frame measurements), the specific core losses W_{Fe} in W/m^3 can be expressed by the theory of the modified Bertotti equation [11]:

$$W_{\mathrm{Fe}} = \left(k_h B_m^2 f + \sigma \frac{d^2}{12} \left(\frac{dB}{dt}(t) \right)^2 + k_e \left(\frac{dB}{dt}(t) \right)^{\frac{3}{2}} \right) k_f , \tag{1}$$

where f is the fundamental frequency, B_m the peak value of the magnetic flux density, σ the conductivity of the material, d the thickness of the lamination, k_h the hysteresis coefficient, k_e is the excess loss and k_f the fill factor coefficient.

Generally, the manufacturer of the magnetic sheets provides the value of iron loss in watts per kilogram for given values of magnetic flux density and frequency. Based on this know-

ledge the loss coefficients (k_e, k_h) can be identified. These coefficients are used to compute iron losses and are reported in Table 2 for M470-50A lamination.

Table 2. Material coefficients for M470-50A lamination

Description		Value	
Hysteresis coefficient	k_h	143	$Ws/T^2/m^3$
Electric conductivity	σ	2.5641 e6	$(\Omega m)^{-1}$
Lamination thickness	d	0.5e-3	m
Excess loss coefficient	k_e	2.6	$W/(Ts^{-1})^{3/2}/m^3$
Packing factor	k_f	0.96	–
Mass density	ρ	7760	kg/m^3

3.2. Eddy-current loss in rotor and PMs

In BLDC motors, iron loss appears not only in the stator but also in the rotor. The rotor of the analysed machine is made of a solid iron. In this case the iron losses are purely the eddy-current losses. A rare earth magnet has relatively high conductivity up to 1.5 μΩm; for electrical motors which work at high speed, the losses generated within magnets should be taken into account due to the risk of demagnetization. PM losses increase related to the speed and over rated speed of the machine will be hazardous to the PM because the increase of losses will raise the temperature of the magnet.

Calculations of the eddy-currents in the PMs are based on the calculation of the distribution of magnetic flux density. Hence, this loss is caused by: winding structure, slot opening size and converter switching frequency. A concentrated winding produces a large amount of current linkage harmonics generated by flux densities travelling across the PMs, causing eddy-currents [12]. This effect can be reduced if the machine uses distributed windings such as the analysed motor. In addition, large stator slot openings cause flux density variations that induce eddy-currents in the PMs. In this paper the rotor iron and magnet loss in Watt unit is computed separately and the Joule losses of PMs and rotor yoke are calculated by Cedrat's Flux3D [13] and is expressed as:

$$W_{\mathrm{PM}} = \iiint_V \mathbf{E} \cdot \mathbf{J}\, dV = \rho \iiint_V J^2\, dV, \tag{2}$$

where $\mathbf{E}$ is the electric field strength, J is the current density within the PM and ρ is the resistivity of the PM ($1.6 \cdot 10^{-6}$ Ωm).

Building the rotor and magnets into multiple segments has been shown to significantly reduce eddy-current loss [14]. In the analysis performed here segmentation into up to six segments is considered (Fig. 4).

The magnetic parts can be glued together. The thickness of the glue is assumed to be 0.1 mm in each bond.

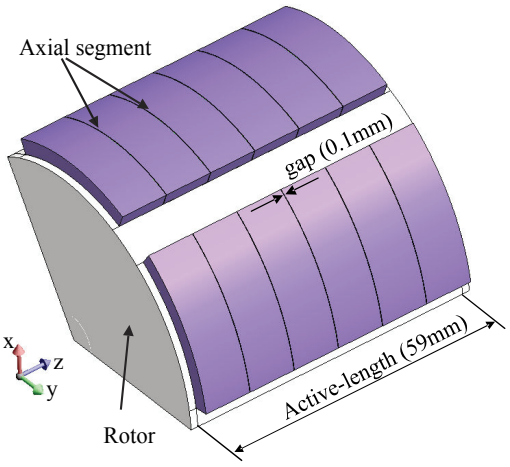

Fig. 4. Magnet pole segmented into 6 pieces over the active length

4. Investigation of BLDC motor with magnet segmentations

The considered motor has a rotational symmetry. Based on the analysis of magnetic flux distribution, it is sufficient to limit the model to one-sixth of the whole motor volume due to the inherent symmetries in both the rotor and stator. Additionally, the 3D mathematical model of a BLDC motor takes into account the end-winding region giving a more accurate solution with regards to loss computing (Fig. 5). The end-winding leakage has influence on magnetic field distribution in the ends of active length. The influence of the end-winding leakage can be weakened, if the rotor length is lower than the stator length (such as in analysed machine).

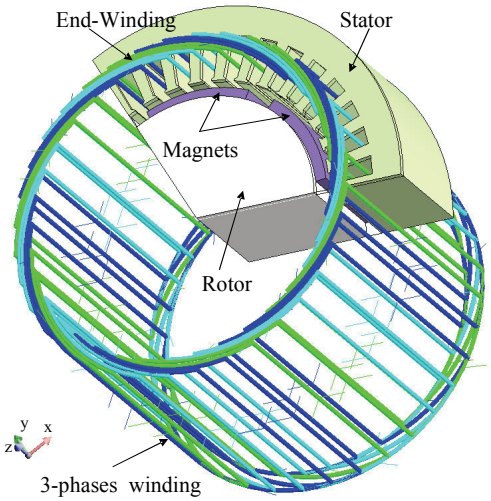

Fig. 5. The 3D FE model, 1/6 of the machine is modelled, by polar and rotational symmetry

In Figure 6, the no-load voltage waveform is computed both without magnet segmentation and when magnet segmentation is employed. The back EMF is slightly lower owing to the

smaller amount of magnets mass. As the number of segments decreases, the maximum decrease in value of back EMF is only about 0.7%. The ripples in the back EMF waveforms are due to the interaction of the rotor design with the stator teeth. Magnet segmentations cause the back EMF ripple to increase, accordingly the torque ripple behaves in the same manner.

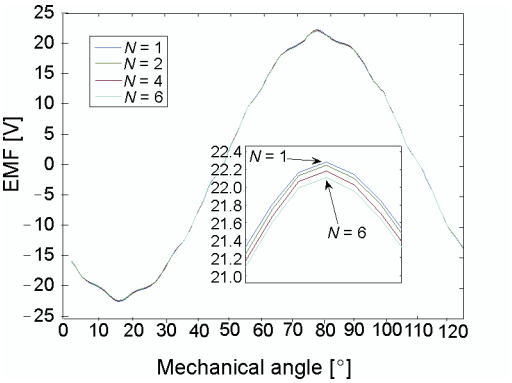

Fig. 6. Back EMF vs. rotor position in mechanical degree due to segmentation magnet at 1000 rpm

Calculation of the torque developed by the motor is performed by the virtual work method [13]. The motor is requiring low level of the torque ripple for low vibration and noise. As it is shown in Fig. 7 the analysed machine produces significant torque pulsations.

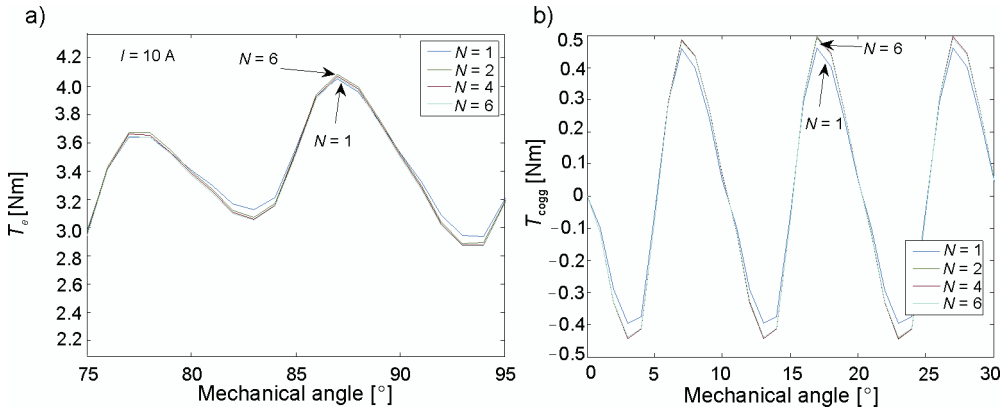

Fig. 7. Electromagnetic torque (a), cogging torque (b) vs. rotor position

Cogging torque minimization of BLDC motors is becoming necessary since its low torque is required in industrial applications. In papers [4, 6, 7] the authors proposed methods to reduce cogging torque. Electromagnetic torque and cogging torque are only slightly influenced by the segmentation of the magnets (Fig. 7a-b). The difference in the peak value of cogging torque between non-segmented magnets and when the magnets are segmented into 6-pieces is approximately 5%. The cogging torque has a tendency to increase due to the rotor construc-

tion, and that is affected by the magnet segmentation. Hence, the air-gap between segmented magnets should be as small as possible.

The iron loss generated in the laminated core pack and in the rotor yoke are presented in Figure 8. Eddy-current loss generated in the rotor yoke is the result of small circulating currents that are induced when the flux density changes in the magnetic material.

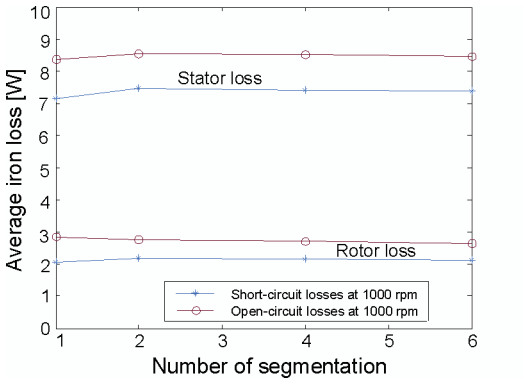

Fig. 8. Iron loss of stator and rotor core vs. number of magnet segments at open circuit and short circuit

The short-circuit iron losses are less than the open-circuit losses due to the weakening at the electromagnetic field by the current flowing in the winding. This effect can be seen in Figure 9 which presents the flux in the air-gap. The air-gap flux under open circuit conditions keeps the flux density profile more rectangular. Figure 9 shows also that under short circuit the flux density form is extremely deformed. Hence, the iron losses under short circuit are less than under open circuit. Table 3 presents a comparison of the calculated iron loss within stator and rotor under open-circuit and short-circuit conditions for a solid magnet (N = 1), two (N = 2), four (N = 4) and six magnet segments (N = 6).

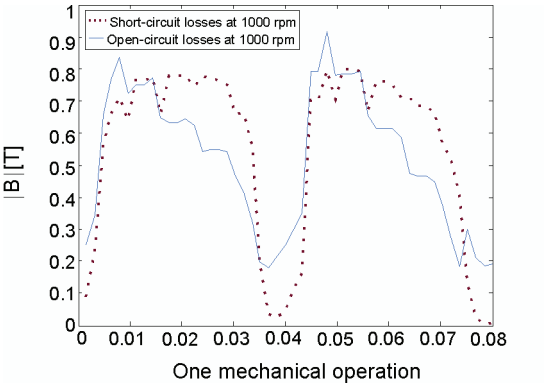

Fig. 9. Flux density in the air-gap for non segmented magnet

In general the rotor eddy-current loss in PMs is relatively low compared to the iron loss. However, it may cause significant heating of the PMs, due to the relatively poor heat dissipation of the rotor that may result in partial irreversible demagnetisation of PMs.

Table 3. Average no-load iron loss of the modified machine at 1000 rpm

Motor version	Rotor iron loss [W]		Stator iron loss [W]	
	Short-circuit	Open-circuit	Short-circuit	Open-circuit
$N = 1$ (prototype)	2.06	2.84	7.16	8.38
$N = 2$	2.18	2.75	7.47	8.56
$N = 4$	2.15	2.71	7.42	8.51
$N = 6$	2.12	2.65	7.38	8.46

As in Figure 10, the PM no-load eddy-current loss is not the dominant part of PM eddy-current losses in the discussed machine with small slot openings and distributed windings. For the maximum number of magnet segments ($N = 6$), the loss is reduced by 66% under short-circuit operation. Hence a reduction in eddy-current loss due to magnet segmentation can be more beneficial for machines which tend to produce more eddy-current loss [1, 10], such as machines using a high numbers of turns per phase, especially machines with concentrated windings and/or machines operated at high speed etc.

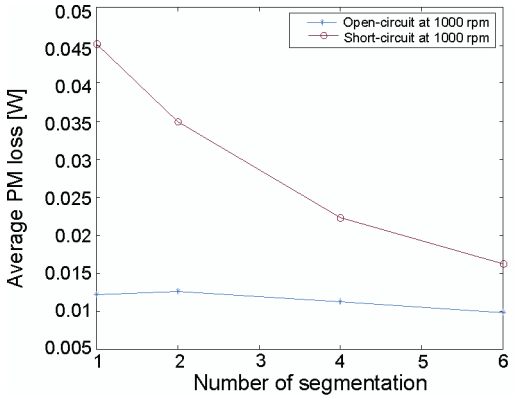

Fig. 10. Eddy-current loss in the PMs vs. segmentation number

Figures 11a and 12a show the distributions of induced current (eddy-current A/m^2) while Figures 11b and 12b show the loss distributions (W/m^3) in the rotor back iron and in a 59 × 30 × 3 mm non-segmented magnet (before magnet segmentation). Due to laminated stator the eddy current losses only appear in the back iron of rotor and magnets. Induced current level for this condition can reach a maximum level $13.294 \cdot 10^6$ A/m^2, while the losses can reach the value of $33.777 \cdot 10^6$ W/m^3. Those maximum values of produced current and losses are within back iron of rotor.

Table 4 and Figure 13 show the calculated eddy-current distributions due to the number of segments. The eddy-current losses in the BLDC motor are reduced by dividing the magnets into segments. If there is necessary to further reduce this undesirable effect and also for the convenience of manufacturing, a magnet can be made of many thin segments, which are electrically insulated from each other. Since the current flux line must close on itself, the

eddy-current circulates confined within segmentation and does not cross over to adjacent ones. And that effect can significantly reduce current loss within PMs.

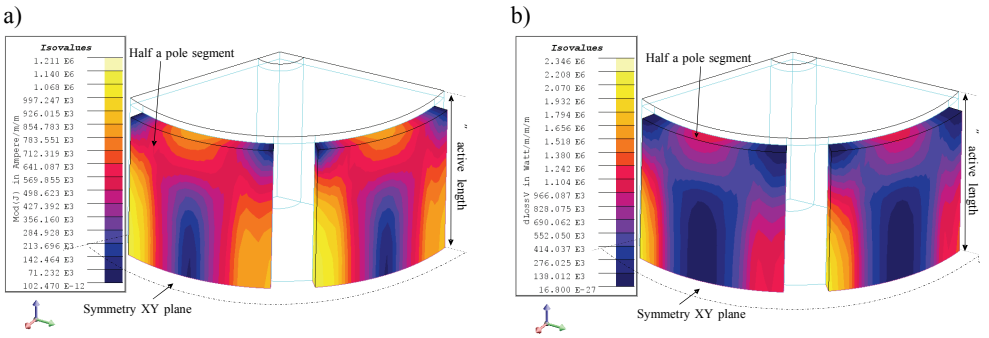

Fig. 11. Induced current density within permanent magnets (a) and loss (b) at mechanical angle 4° under short-circuit before magnet segmentation

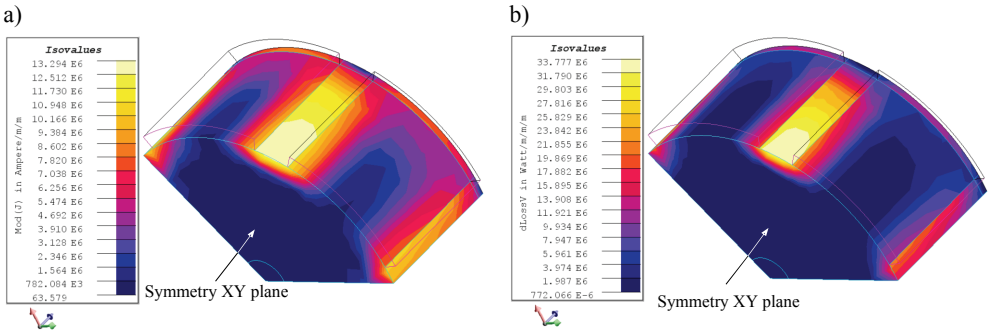

Fig. 12. Induced current density within back iron of rotor (a) and loss (b) at mechanical angle 4° under short-circuit before magnet segmentation

Table 4. Average no-load PM loss of the modified machine at 1000 rpm

Motor version	PM loss [%] relative to non-segmented magnets		PM loss [W]	
	Short-circuit	Open-circuit	Short-circuit	Open-circuit
$N = 1$ (prototype)	100%	100%	0.0452	0.0122
$N = 2$	77%	100%	0.0349	0.0126
$N = 4$	51%	92%	0.0223	0.0112
$N = 6$	34%	81%	0.0162	0.0098

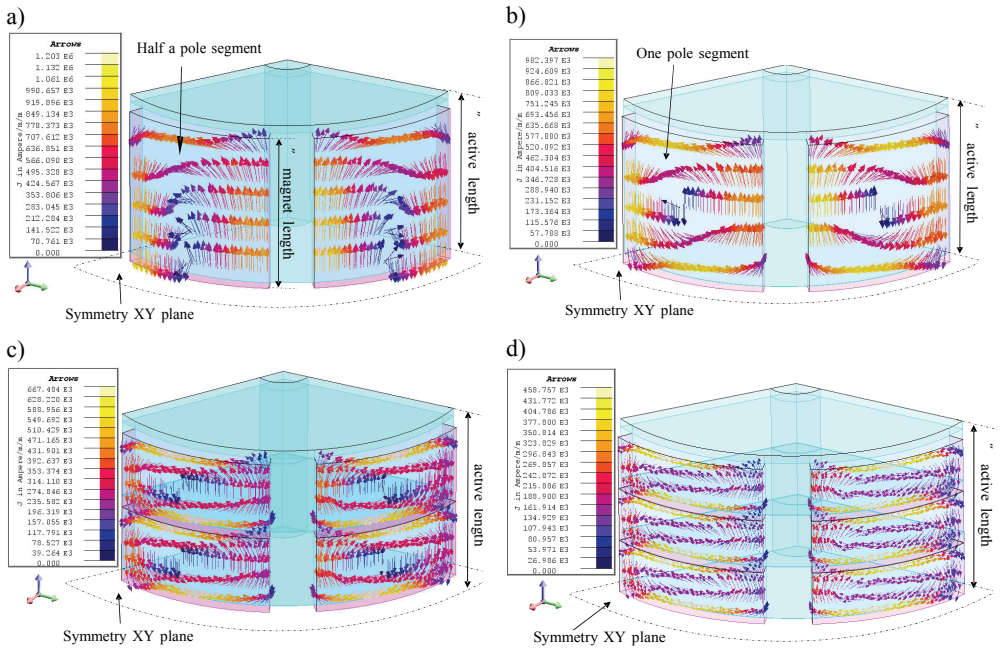

Fig. 13. Eddy-current loss distribution in the PMs for $N = 1$ (a), $N = 2$ (b), $N = 4$ (c) and $N = 6$ (d) at 1000 rpm and short-circuit

5. Investigation of BLDC motor with a discrete skewed magnet

Magnet segmentation was shown to reduce heat loss, however a side-effect of this was a significant increase in cogging torque amplitude. The act of segmenting magnets in order to limit heat losses opens up the possibility of reducing the cogging torque amplitude simultaneously. By introducing a discrete skew angle between magnet segments we can limit the effect of two problems simultaneously: heat losses caused by eddy currents in magnets and cogging torque amplitude.

Figure 14 shows how the segmentation is achieved.

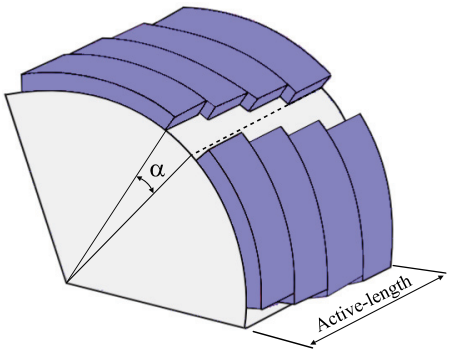

Fig. 14. Rotor with discrete skewing of the magnets divided into 4 segments where $\alpha = 10°$

In this particular structure of rotor the cogging effect can be significantly reduced when permanent magnets without any segmentation are replacing with a discrete skew along the machine length. In this case, the rotor magnets are divided into 4 identical slices with α – the angular displacement (discrete skew angle) equal to 10°. Due to the skewed magnets an accurate FE analysis can only be performed with a three dimensional FE model, because flux distribution is not uniform down the length of the rotor due to the skewing.

The angular displacement of a magnet segment is defined as the angle between the first and last segment of a pole, here from 0° to 10°.

5.1. Cogging torque

Figure 15a presents maximum values of cogging torque $T_{coggmax}$ versus angular displacement of magnet segments. For each quantity of segments there is a shift in optimum skew angle where the minimum amplitude of the cogging torque occurs. Increasing the number of magnet segments causes the skew angle to increase. In the case where the magnet is divided into two segments (N = 2), three segments (N = 3) and four segments (N = 4) the optimum skew angle of segments is 5°, 7° and 8°, respectively. Figure 15b compares cogging torque variations for these chosen magnet segment angle displacements. The highest reduction in the cogging torque was achieved with four magnet segments (T_{coggmax} = 0.0531 Nm) and for three magnet segments (T_{coggmax} = 0.0564 Nm).

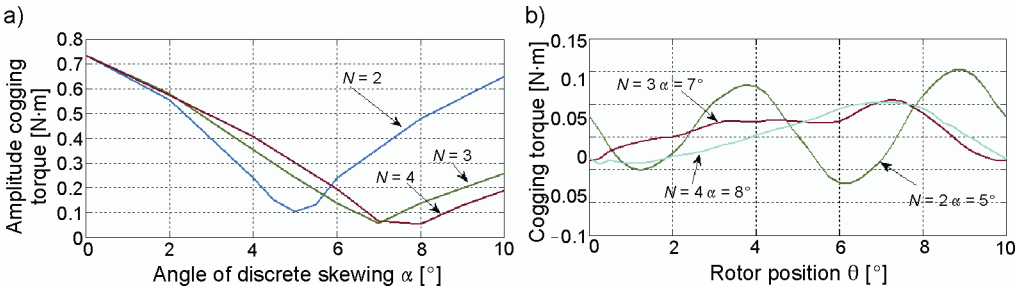

Fig. 15. Angular PM slices displacement – α of maximum cogging torque (a) and angular variation of cogging torque (b) for various shapes of rotor with skewed magnets

5.2. Electromagnetic torque

According to Figure 16, changing the number of magnet segments leads to a change in electromagnetic torque amplitude T_{emax}. Reduction of cogging torque amplitude causes a concurrent decrease in the maximum value of the electromagnetic torque achieved and that is a disadvantageous effect. The minimum values of the cogging torque (Fig. 15a) and T_{emax} (Fig. 16) occur at the same value of α, this correlation is expected as the two properties are interrelated.

Figure 17a shows average value of the electromagnetic torque T_{eav} versus angle of discrete skew for different magnet segmentation numbers. Additionally, angular variations of the electromagnetic torque T_e at the rated current both for the basic (unsegmented) and segmented

motor versions are depicted in Figure 17b. The increase in the magnet angular displacement causes a decrease in the average value of electromagnetic torque.

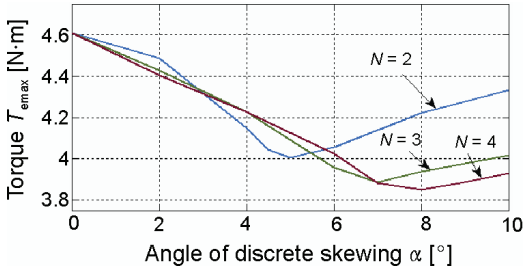

Fig. 16. Angular PM slice displacement (α) of the maximum electromagnetic torque for various shapes of rotor with skewed magnets

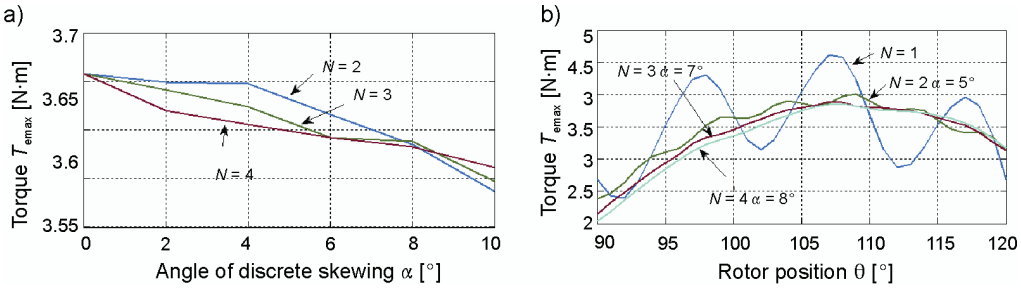

Fig. 17. Angular PM slice displacement – α of average electromagnetic torque (a) and angular variations of electromagnetic torque (b) for various shapes of rotor with skewed magnets

6. Conclusion

The computed PM eddy-current loss in the considered machine with the segmented PM poles is significantly lower (about 66% under short and 19% under open circuit) compared to the machine without the segmentation used; however, the effect of segmentation is to generate almost the same range of iron losses (the loss at short and open circuit was separated by calculating the stator loss and PMs eddy-current losses). The proposed approach to reduce eddy-current loss is most beneficial for BLDC machines with high number of turns per phase, concentrated windings or machines with a high fundamental frequency, e.g. high speed operation and/or high pole number, machines with large slot openings and a high power density. In this case, axial-segmentation of the magnet reduced loss, and kept the same range of EMF value and did not increase significantly a cogging torque. The presented method for reduction of the cogging torque can be applied in different types of electrical machines with the surface mounted magnets. The reduction of the cogging torque using discrete skew magnets method with respect to the basic version of BLDC motor is achieved up to 90%.

References

[1] Chen Y., Zhu Z.Q., Howe D., Gliemann J.H., *Rotor eddy current loss in single-phase permanent magnet brushless DC motor*. Industry Applications Conference, 42nd IAS Annual Meeting, Conference Record of the 2007 IEEE, pp. 537-543 (2007).

[2] Ionel D.M., Popescu M., Cossar C. et al. *A general model for estimating the laminated steel losses under PWM voltage supply*. IEEE Transactions on Industry Applications 46(4): 1389-1396 (2010).

[3] Boglietti A., Cavagnino A., Ionel D.M. et al. *A general model to predict the iron losses in inverter fed induction motors*. Energy Conversion Congress and Exposition, ECCE 2009, IEEE, pp. 1067-1074 (2009).

[4] Mlot A., Lukaniszyn M., *Optimization of the PM array of brushless DC motor for minimum cogging torque*. Przegląd Elektrotechniczny 12: 68-70 (2008).

[5] Lukaniszyn M., Jagiela M., Wrobel R., *Optimization of permanent magnet shape for minimum cogging torque using a genetic algorithm*, IEEE Transactions on Magnetics. 40(2): 1228-1231 (2004).

[6] Korkosz M., Mlot A., *Torque ripple reduction by using multi-slice FE modelling of brushless DC motor with skewed magnets*, Zeszyty Problemowe – Maszyny Elektryczne 86: 105-108 (2010), (in Polish).

[7] Lukaniszyn M. Mlot A., *Torque characteristics of BLDC motor with multipolar excitation*. The International Journal for Computation and Mathematics in Electrical and Electronic Engineering, COMPEL 28(1): 178-187 (2009).

[8] Cassat A., Espanet C., Wavre N., *BLDC motor stator and rotor iron losses and thermal behavior based on lumped schemes and 3D FEM analysis*. Industry Applications Conference 4: 2469-2476 (2002).

[9] Kohan N.A., Abbaszadeh K., *Influence of nonsinusoidal flux waveform on transformer design methodology*. 1st Power Electronic & Drive System & Technologies Conference, pp. 57-62 (2010).

[10] Chen Y., Pillay P., *An improved formula for lamination core loss calculations in machines operating with high frequency and high flux density excitation*. Industry Applications Conference, 2: 759-766 (2002).

[11] Bertotti G., *General properties of power losses in soft ferromagnetic materials*. IEEE Transactions on Magnetics 24(1): 621-630 (1988).

[12] Benarous M., *Investigation of rotor loss due to current communication in a permanent magnet brushless DC motor*. Power Electronics, Machines and Drives. The 3rd IET International Conference, pp. 546-550 (2006).

[13] Cedrat, Flux3D, User's Guide 3 (2008).

[14] Yamazaki K., Fukushima Yu., *Effect of eddy-current loss reduction by magnet segmentation in synchronous motors with concentrated windings*. Electrical Machines and System, ICEMS, pp. 1-6 (2009).

[15] Mlot A., Korkosz M., Lukaniszyn M., *Analysis of Iron and Eddy-Current Loss in Low-Power BLDC Motor with Magnet Segmentations*, Zeszyty Problemowe – Maszyny Elektryczne 93: 59-64 (2011).